An improved global zenith tropospheric delay model GZTD2 considering diurnal variations

YiBin Yao[1,2,3], YuFeng Hu[1], Chen Yu[1], Bao Zhang[1], JianJian Guo[1]

[1]*School of Geodesy and Geomatics, Wuhan University,* 129 *Luoyu Road, Wuhan* 430079*, China. E-mail:* *ybyao@whu.edu.cn*

[2]*Key Laboratory of Geospace Environment and Geodesy, Ministry of Education, Wuhan University,* 129 *Luoyu Road, Wuhan* 430079*, China*

[3]*Collaborative Innovation Center for Geospatial Technology,* 129 *Luoyu Road, Wuhan* 430079*, China*

Abstract--The zenith tropospheric delay (ZTD) is an important atmospheric parameter in the wide application of global navigation satellite systems (GNSS) technology in geoscience. Given that the temporal resolution of the current Global Zenith Tropospheric Delay model (GZTD) is only 24 h, an improved model GZTD2 has been developed by taking the diurnal variations into consideration and modifying the model expansion function. The data set used to establish this model is the global ZTD grid data provided by Global Geodetic Observing System (GGOS) Atmosphere spanning from 2002 to 2009. We validated the proposed model with respect to ZTD grid data from GGOS Atmosphere, which was not involved in modeling, as well as International GNSS Service (IGS) tropospheric product. The obtained results of ZTD grid data show that the global average Bias and Root Mean Square (RMS) for GZTD2 model are 0.2 cm and 3.8 cm respectively. The global average Bias is comparable to that of GZTD model, but the global average RMS is improved by 3 mm. The Bias and RMS are far better than EGNOS model and the UNB series models. The testing results from global IGS tropospheric product show the Bias and RMS (-0.3 cm and 3.9 cm) of GZTD2 model are superior to that of GZTD (-0.3 cm and 4.2 cm), suggesting higher accuracy and reliability compared to the EGNOS model, as well as the UNB series models.

Key Words—Zenith tropospheric delay; GGOS Atmosphere; IGS; Diurnal variation; GZTD2 model.

1. Introduction

Radio space-based geodesy techniques suffer from atmosphere propagation delays, of which the ionospheric delay can be largely eliminated by iono-free carrier phase combination techniques (Spilker 1980), and then the tropospheric delay becomes the main error source. In general, we project the slant delay to zenith direction with mapping function in GNSS navigation and positioning, so modeling the ZTD is a common method to reduce the tropospheric influence on signal travelling. In order to improve the accuracy and efficiency of the application in earth science based on space geodesy techniques, a reliable tropospheric delay model is required.

Some tropospheric delay models are developed to mitigate the tropospheric delay. The traditional models like the Hopfield model (Hopfield 1969), Saastamoinen model (Saastamoinen 1973) and Black model (Black 1978) require real-time meteorological data to reach a correction accuracy better than 10 cm. Given the location and time information, the UNB series models (Collins and Langley 1997, 1998; Leandro et al. 2006, 2008) and EGNOS model (Dodson et al. 1999; Penna et al. 2001; Ueno et al. 2001) use the empirical meteorological parameters in the form of the latitude band table to estimate the ZTD with an accuracy of about 5 cm, while the IGGTrop model (Li et al. 2012) is based on the empirical three-dimensional parameters in the form of the grids to calculate the ZTD with an accuracy of about 4 cm. However the IGGTrop model needs a large number of parameters. Then Li Wei et al. (2015) developed the new versions of IGGtrop named IGGtrop_ri (i = 1, 2, 3) by simplifying the algorithm and lowering the resolution, which substantially reduce the required numbers with a similar accuracy. Krueger (2004;2005) and Schüler (2014) obtained the annual and diurnal coefficients for underlying parameters by fitting every grid point's meteorological parameters time series of the National Centers for Environmental Prediction (NCEP) atmospheric data, and established two global tropospheric delay models — TropGrid and TropGrid2 . The correction accuracy of TropGrid2 is 3.8 cm. Böhm et al. (2015) proposed Global pressure and temperature 2 wet (GPT2w) as an extension to GPT2 (Lagler et al. 2013) with an improved capability to determine zenith wet delays in blind model. The GPT2w model accounts for the annual and semiannual variations of meteorological parameters, and the validation with IGS data and an extended validation with ray-traced delays (Möller et al. 2014) show a high accuracy of about 3.6 cm for GPT2w. However, GPT2w has numerous parameters for storage like the above grid models such as IGGTrop series models and TropGrid series models.

Yao et al. (2013) established a global non-meteorological parameters tropospheric delay model GZTD (Global Zenith Tropospheric Delay) based on spherical harmonics using the global zenith tropospheric delay grid data provided by Global Geodetic Observing System (GGOS) Atmosphere. The harmonic function including three terms (mean, annual and semi-annual) is used to fit the ZTD time series from 2002 to 2009 for each grid, then the fitted coefficients of all the grids are expanded with a 10-order and 10-degree spherical harmonics. Its modeling approach was very simple, and the overall accuracy of 4.2 cm was similar to the IGGtrop on a global scale, but the required parameters were reduced greatly to about 600. GZTD model is constructed by global daily average ZTD grid data and the model parameters were expanded with a low order spherical harmonics, whose temporal resolution is only one day in theory and spatial resolution is low.

In this paper, using the ZTD grid data provided by the GGOS Atmosphere, the diurnal variations in ZTD were analyzed to prove the practical necessity for temporal resolution improvement of GZTD model. Then on the basis of GZTD model and taking the diurnal variations into consideration and modifying the expansion function, we developed an improved global non-meteorological parameters ZTD model — GZTD2. The data set used to establish this model is the global ZTD grid data provided by the GGOS Atmosphere from 2002 to 2009. Using ZTD grid data obtained from GGOS Atmosphere and tropospheric product (Buyn et al. 2009) provided by IGS for model validation, the accuracy of GZTD2 model is superior to that of GZTD model, and this model performs much better than other commonly used models such as EGNOS model and UNB series models.

2. The new tropospheric delay model

The GGOS Atmosphere is a project that aims to establish atmospheric models, which has been carried out at Vienna University of Technology and has been funded by the Austrian Science Fund (Böhm & Schuh 2013). It provides grid data of global zenith delays (including zenith hydrostatic delay (ZHD) and zenith wet delay (ZWD)) with temporal resolution of 6 hours (0:00, 6:00, 12:00, 18:00UTC) and spatial resolution of 2.5°×2° (lon×lat), which are derived from the reanalysis data (Uppala et al. 2005) provided by the ECMWF. The ZTD grid data can be obtained by simply adding up the ZHD and the ZWD at the same point and time. In this paper, the research about model establishment is based on the ZTD grid data.

2.1 Diurnal variations in ZTD

Yao et al. (2013) developed a new global zenith tropospheric delay model (GZTD), which is based on spherical harmonics without using meteorological parameters. GZTD model depends on four parameters: the day of year (doy), the latitude, the longitude and the height; and the overall accuracy is up to centimeter level. However, the algorithm of GZTD model only considers the annual and semiannual cycles in ZTD and the establishment of GZTD model is based on the daily average of global grid ZTD data, hence the temporal resolution of GZTD model is one day (24 h) in theory. We randomly selected six grid points which represent the regions in low, middle and high latitude in both the southern and northern hemispheres respectively, and applied GZTD model to estimate the ZTD at four moments (0:00,6:00,12:00,18:00 UTC) of the first day of the year (doy) in 2010, then compared the GZTD model estimations with the corresponding data from GGOS. The results are shown in Figure 1.

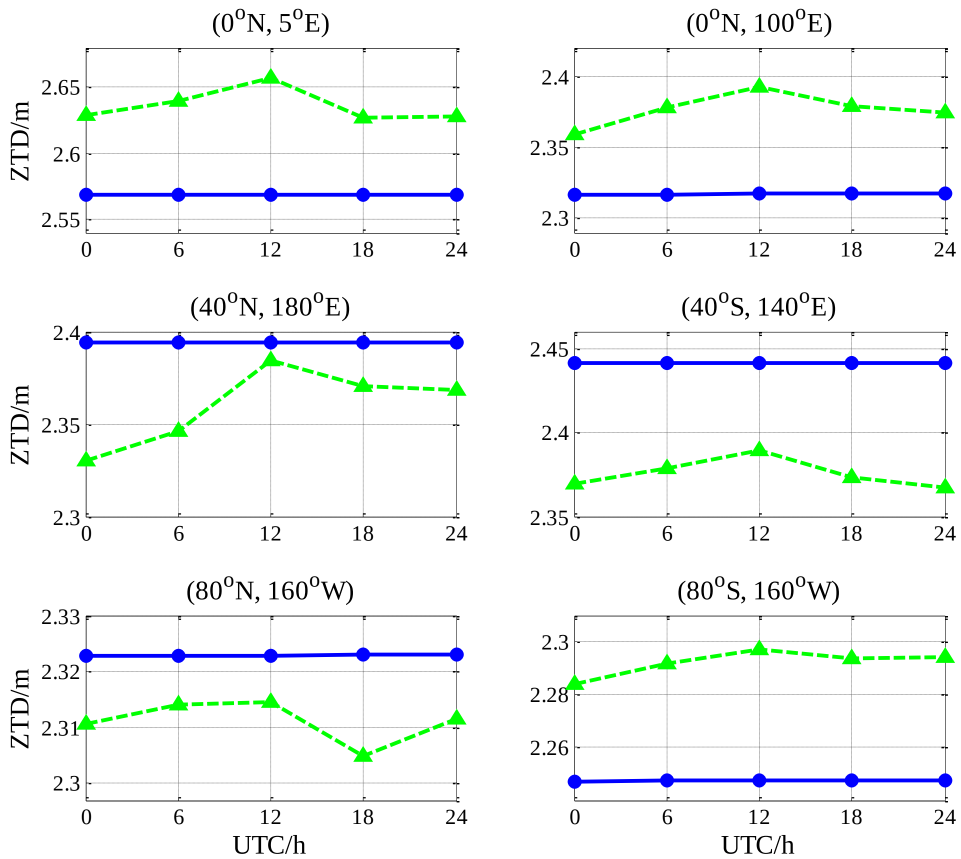

Figure 1. GZTD model estimates(blue ○) and corresponding GGOS grid values (green △) at the first doy of 2010

We can see clearly from Figure 1 that the ZTD estimates of GZTD model can almost be fitted with a straight line parallel to the time axis which only varies about 1 mm in a single day. The real variations of GGOS grid ZTD data are mostly up to centimeter level, which is one order larger than the variations of GZTD model estimates. Furthermore, we calculated the mean diurnal ZTD values of these six GGOS grid points over the whole 2010 year (Figure 2), and the significant signal of diurnal variation can be seen at all these six grid points .We can draw a conclusion that GZTD model could not reflect the characteristic of diurnal variations in ZTD, so the model estimations nearly have no difference when doing calculation with real value or corresponding integer value of the input doy. Therefore, it is necessary to improve the temporal resolution of GZTD model to reflect diurnal variations. It should be noted that Jin et al. (2009) has investigated the diurnal and semidiurnal variations in ZTD which obtained from a decade of global GPS observations, and thought that the atmospheric tides were the major driver of these variations after finding the general similarities of diurnal variations between ZTD and pressure. However, the semidiurnal variations could hardly be described because of the low temporal resolution (6 h) of GGOS ZTD data, so we didn't consider the semidiurnal components of ZTD in modeling in the following section.

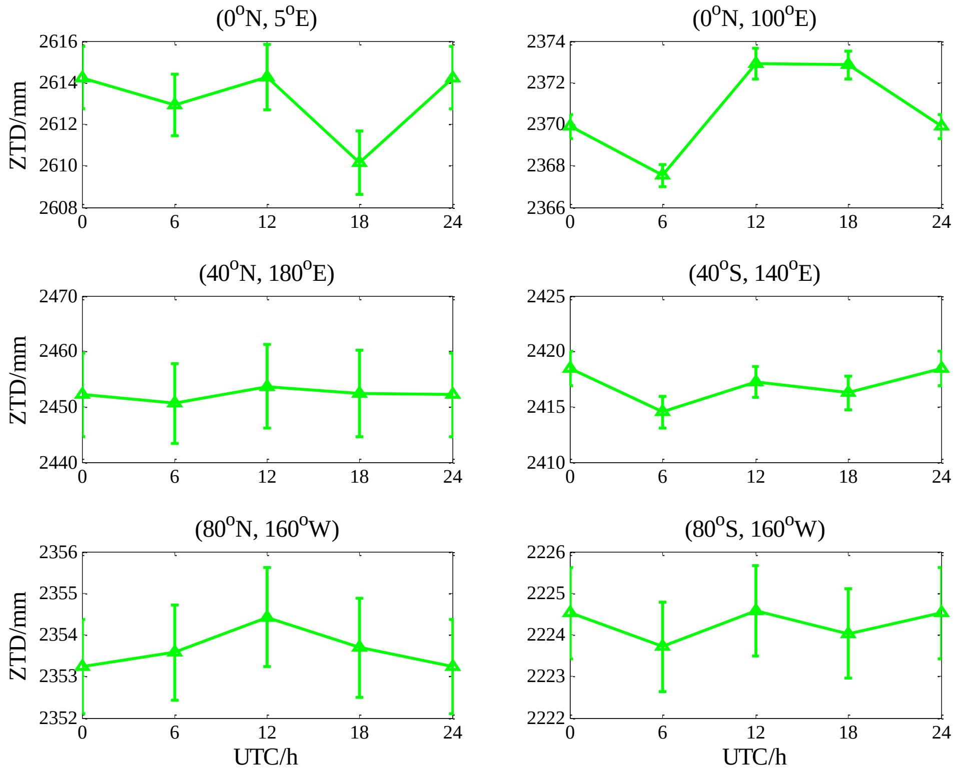

Figure 2. Mean diurnal ZTD values of GGOS grid points with error bars denoting the standard deviations from the average over the 2010 year

2.2 Establishment of GZTD2 model

According to the previous researches conducted by Jin et al. (2007) and Yao et al. (2013), ZTD decreases exponentially with increasing height, is featured by one-year periodicity and half-year periodicity, and has a strong correlation with latitude. Based on these characteristics of ZTD, we took diurnal periodic variations into consideration to develop an improved model GZTD2. The expression of GZTD2 model is as follows:

$$\mathrm{ZTD} = \left[a_0 + a_1 \cos(2\pi \frac{\mathrm{doy} - a_2}{365.25}) + a_3 \cos(4\pi \frac{\mathrm{doy} - a_4}{365.25}) + a_5 \cos(2\pi \frac{\mathrm{hod} - a_6}{24}) \right] \exp(\beta h)$$

(1)

Where,

$$a_i = \sum_{n=0}^{18}\sum_{m=0}^{n} \mathrm{P}_{nm}(\sin\varphi)\cdot[\mathrm{A}_{nm}^{i}\cos(m\lambda)+\mathrm{B}_{nm}^{i}\sin(m\lambda)] \qquad (i=0,1,\cdots,6) \tag{2}$$

In equation(1), doy is the day of the year; hod is the UTC time; h is the height (altitude); a_0 is the annual mean of ZTD on the mean sea level (MSL); a_1 is the annual variation amplitude of ZTD; a_2 is the initial phase of annual variation; a_3 is the semiannual variation amplitude of ZTD; a_4 is the initial phase of semiannual variation; a_5 is the diurnal periodic variation amplitude of ZTD; a_6 is the initial phase of diurnal variation; $\beta = -0.00013137$ is the constant to reduce the ZTD at height to the MSL, which was determined by Yao et al. (2013) by fitting the global GGOS grid ZTD via exponential function with respect to height; P_{nm} are the Legendre polynomials; φ is the latitude of grid point; λ is the longitude of grid point; A_{nm}^{i} and B_{nm}^{i} are the coefficients of spherical harmonics determined by least square optimization.

For each grid-point-specific ZTD time series derived from GGOS Atmosphere, we used equation (1) to fit them to temporal coefficients at MSL. Our previous GZTD model only accounts for the annual and semi-annual variations of ZTD, whose first equation is similar to equation (1) but without the fourth term (diurnal term) on the right of equation (1). However, there are seven coefficients for each grid, which need large storage space on global scale. Then referring to the idea of spherical harmonics used in GPT (Böhm et al., 2007), we used equation (2) to express the temporal coefficients (mean, annual terms et al) of all grids as a function of location (latitude, longitude and height), thus reducing the parameters. In contrast with the GZTD model established using daily average global ZTD data, we utilized the ZTD time series data of four moments per day (0:00, 6:00, 12:00, 18:00UTC) from 2002 to 2009, provided by GGOS Atmosphere, to fit ZTD values to obtain temporal variation parameters via equation (1), then expanded these parameters with a 18-order and 18-degree spherical harmonic function (equation (2)), respectively. The expansion equation of GZTD model is a 10-order and 10-degree spherical harmonic function which is 8 less order and degree than equation (2). We used this spherical harmonic function instead of the 10-order and 10-degree function adopted in GZTD model because it is not sufficient to apply the previous 10 order function for the expansion of the temporal variation parameters with relatively high resolution. The number of order and degree of spherical harmonics determine the horizontal resolution of model. However, higher order and degree bring more parameters for model. The 10 spherical harmonics adopted by GZTD result in a resolution of about 18°, which is too low for GZTD2 model to reflect the small diurnal variations. To keep a balance between the resolution and number of parameters, we used 18 spherical harmonics for GZTD2 whose resolution is about 10°.

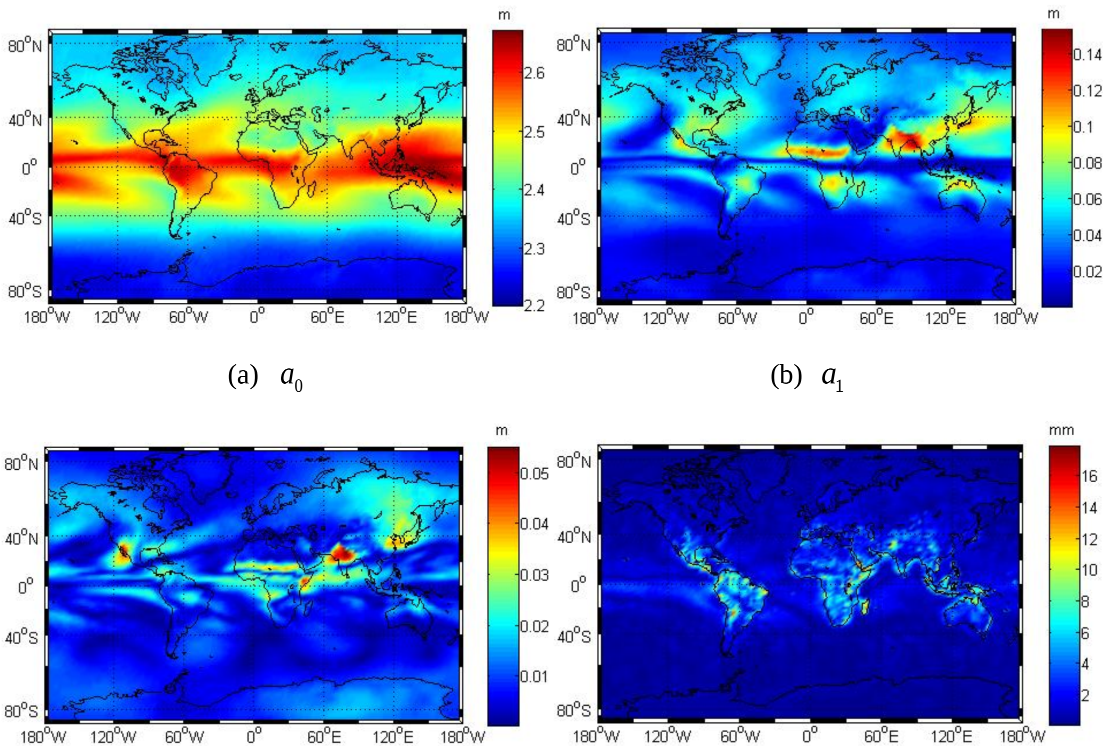

(a) a_0 (b) a_1

(c) a_3 (d) a_5

Figure 3. The global distribution of the annual mean ZTD on MSL (a) , the annual variation amplitude (b), the semiannual variation amplitude (c), and the diurnal variation amplitude (d)

Figure 3 shows the global distributions of the annual mean of ZTD on MSL and amplitude parameters after fitting by equation (1). As can be seen from Figure 3a, the coefficient a_0 in low latitudes, especially, near the equator, are significantly larger than that in high latitudes, and the distribution in the Southern Hemisphere is more uniform than that in the Northern Hemisphere; These results are mostly in agreement with the results of Li et al. (2012) and Yao et al. (2013). For the sawtooth shape in the 40 °N-40 °S region, Yao et al. (2013) found this shape appear in coastal areas and is consistent with the directions of equatorial trade winds, so they assumed that the distributions of ZTD are effected by some physical impacts such as terrains and heat circulation. Compared with the previous discovery, the sawtooth shape in Figure 3a is more evident, indicating that GZTD2 model incorporates these physical impacts. Figures 3b and 3c show the global distributions of annual amplitude and semiannual amplitude respectively, both of which are more uniform in the Southern Hemisphere than that in the Northern Hemisphere, which is probably due to the fact that most parts of the Southern Hemisphere are covered by oceans, while the Northern Hemisphere has many seacoast regions which lead to relatively complex spatial variation.

Figure 3d shows the global distribution of diurnal variation amplitudes. It can be seen that diurnal variation amplitudes are less than 3 mm in most parts of the world, but up to centimeter in some low-latitude equatorial areas such as Central America, South America, central Africa and tropical Asia, indicating notable diurnal variations in these areas. The distribution characteristics of diurnal variation amplitudes is similar to the results of Jin et al. (2009). So taking these diurnal variations into consideration in GZTD2 model is quite reasonable and necessary.

The GZTD2 model only needs doy, UTC time, latitude, longitude and height as input parameters in practical application. GZTD2 uses equation (2) to derive temporal parameters a_0, a_1, a_2, a_3, a_4, a_5, a_6, which are then entered into equation (1) together with the doy to get the ZTD at MSL. The realization of GZTD2 model is simple with a few parameters, and the calculation is convenient without inputting any real-time meteorological parameters. Table 1 summarizes the main improvements and features of the newly suggested model compared to the GZTD model.

Table 1. Improvements of GZTD2 with respect to GZTD

	GZTD	GZTD2

Data	Daily average ZTD grid data from GGOS: 2002~2009	ZTD grid data with a resolution of 6 h from GGOS: 2002~2009
Representation	Spherical harmonics up to degree 10 and order 10	Spherical harmonics up to degree 18 and order 18
Temporal variability	Mean, annual, and semi-annual terms	Mean, annual, semi-annual and diurnal terms
Horizontal resolution	About 18 °	About 10 °

3. Validation and Analysis of GZTD2 model

To analyze the effectiveness and reliability of the new model and verify its accuracy and stability on global scale, as well as to compare it with the GZTD model, this section will exploit some data sources to conduct model validation. Two kinds of data sources are used here, the first is ZTD grid data from GGOS Atmosphere which is not used in modeling. The other is tropospheric product data provided by IGS. The accuracy is characterized with the average deviation (Bias) and root mean square (RMS) which are usually used for model validation (Yao et al., 2013; Li Wei et al., 2015; Böhm et al., 2015). The expressions of Bias and RMS are:

$$Bias = \frac{1}{n}\sum_{i=1}^{n}(ZTD_i^M - ZTD_i^0) \tag{3}$$

$$RMS = \sqrt{\frac{1}{n}\sum_{i=1}^{n}(ZTD_i^M - ZTD_i^0)^2} \tag{4}$$

Where ZTD_i^M is the value estimated by model and ZTD_i^0 is the reference value.

3.1 Validation with GGOS Atmosphere ZTD grid data

Data provided by GGOS Atmosphere from 2002 to 2009 are involved in modeling, so we used the data of 2010 to test it. Since the resolution of ZTD grid data is 2 °× 2.5 °, the total number of grid points is 13,104. Treating the ZTD data at 0:00, 6:00, 12:00 and 18:00 UTC of everyday on each grid point as the reference values, we calculated the bias and RMS of GZTD2, GZTD, EGNOS, UNB3 and UNB3m models. Statistical analyses are shown in Table 2.

Table 2. Modeling errors of different models validated by GGOS data

	Bias (in cm)			RMS (in cm)		
	Mean	Min	Max	Mean	Min	Max
GZTD2	0.2	-3.7	6.2	3.8	0.9	8.3
GZTD	0.2	-5.4	8.0	4.1	1.1	9.5
UNB3m	3.3	-7.2	16.0	6.4	1.3	16.5
UNB3	4.5	-7.0	16.7	7.0	1.1	16.9
EGNOS	4.5	-9.6	17.7	7.2	1.0	18.1

As can be seen from Table 2, for the total 13104 points involved in the global validation, GZTD2 model's mean Bias is 0.2 cm with a maximum of 6.2 cm, and the average of RMS is 3.8 cm with a maximum of 8.3 cm, significantly better than the EGNOS and UNB series models, and the RMS is reduced by 3 mm compared with that of GZTD model. UNB3m model's accuracy is about 1 cm better than UNB3 and EGNOS models, so we only chose UNB3m as the representative of commonly used model in our following comparison analysis. Figure 4 shows the global distributions of Bias and RMS of the three models.

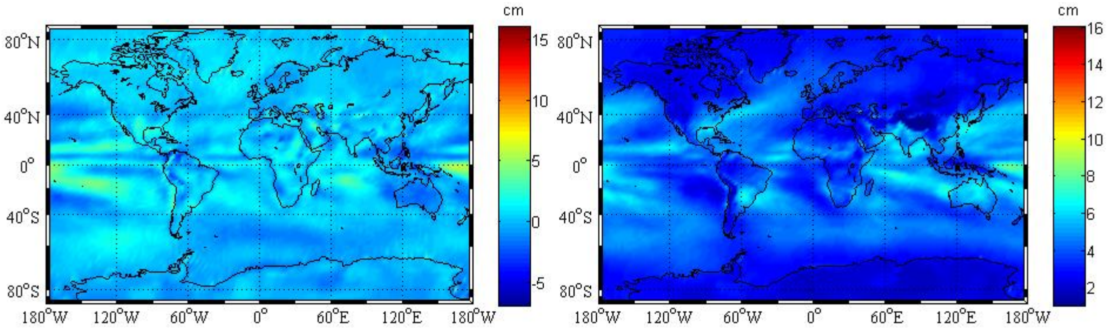

GZTD2 Bias GZTD2 RMS

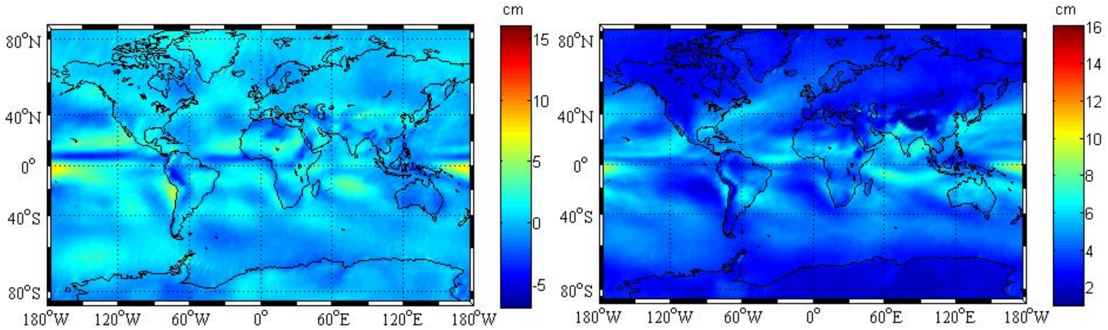

GZTD Bias GZTD RMS

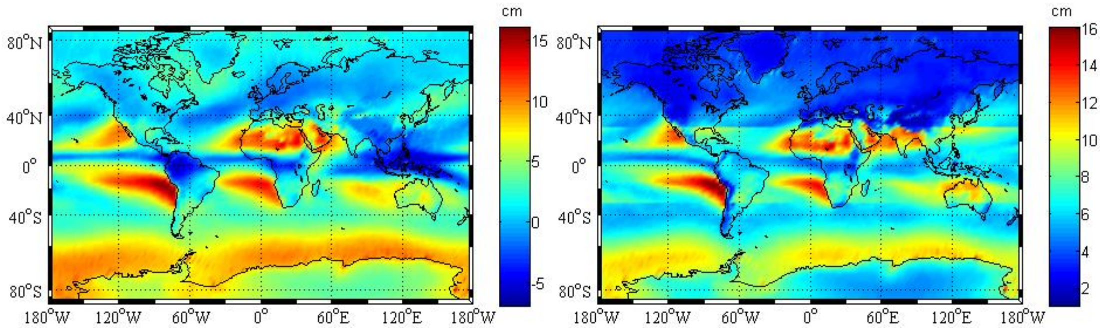

UNB3m Bias UNB3m RMS

Figure 4. Global distribution of Bias and RMS of different models

As can be seen from Figure 4, compared with the other two models, the new model has better accuracy in the world wide scale, and the accuracy of the areas where lager errors appear improves significantly. Compared with GZTD model, GZTD2 model improves the accuracy in the equator area. Obviously, all these three models have suffered large errors in the Pacific Ocean near the equator and Indian Ocean. These areas are near the equator where the deep moist convection effects related to the change of ZTD are more intense (Trenberth et al. 2005; Pramualsakdikul et al. 2007), so the weather change in these areas are more complex compared with other areas, resulting in difficulty for modelling tropospheric delay. In addition, GZTD2 and GZTD model are comparable in Northern and Southern Hemispheres, but the UNB3m model's accuracy is obviously lower in the Southern Hemisphere, this is because the UNB3m model is based on the assumptions that tropospheric delay is symmetrical with equator (Leandro et al., 2006). In fact, this assumption is not reasonable enough and the modeling data source are derived from North America, so the accuracy of the model is higher in North Hemisphere, especially in Northern America.

3.2 Validation with IGS tropospheric delay data

IGS has provided final troposphere products with a temporal resolution of 5 minutes since 1998. In 2010, some IGS sites have the severe problem of ZTD data missing. For a convinced validation, only the IGS sites with at least 120 days (approximately a third of the year) of tropospheric delays are selected. Consequently, there are 362 IGS sites selected in 2010 to verify the accuracy of GZTD2 model, and the distribution of IGS sites is shown in Figure 5. The uncertainties of the ZTD products are very small (see Figure 5) with a mean value of 1.5 mm, indicating high quality of the ZTD products. Considering the ZTD products of IGS sites as true value, we tested and analyzed the ZTD estimates of GZTD2 model, GZTD model, EGNOS model and UNB series models. The Bias and RMS statistical results are shown in Table 3.

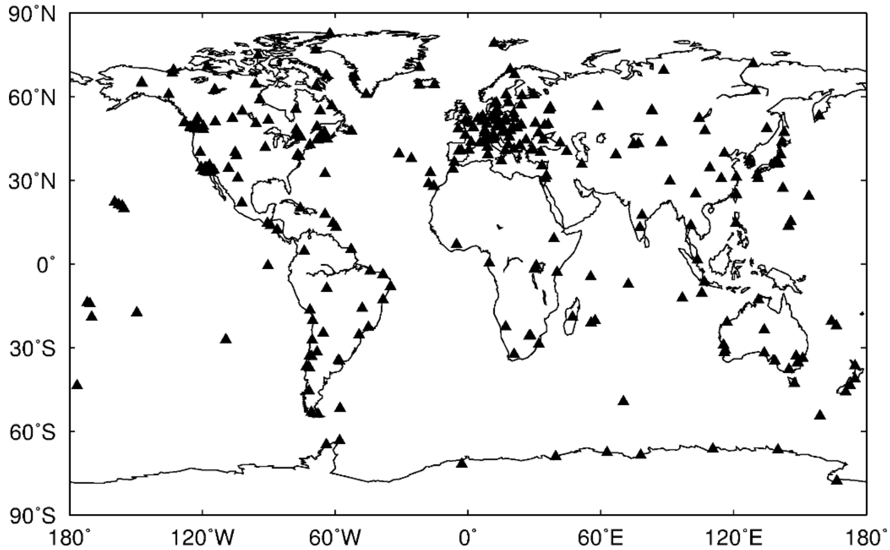

Figure 5. Distribution of global IGS sites involved in validation

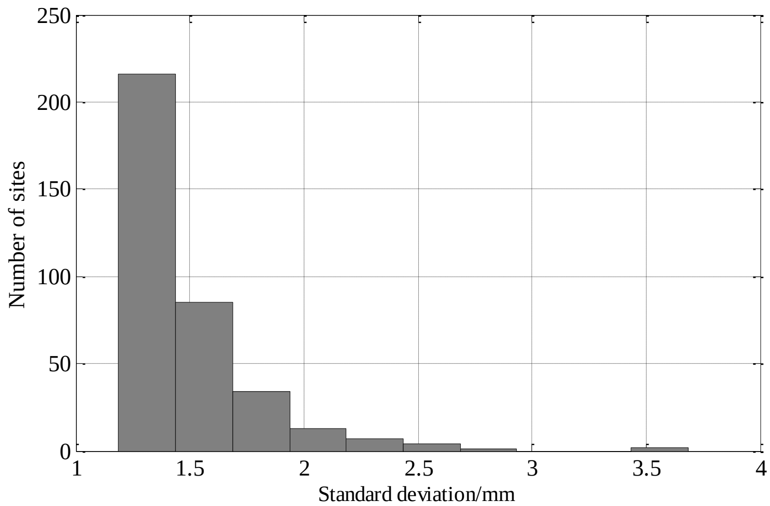

Figure 6. Histogram of uncertainty of ZTD at selected IGS sites

Table 3. Error of different considered models versus IGS data

	Bias (in cm)			RMS (in cm)		
	Mean	Min	Max	Mean	Min	Max
GZTD2	-0.3	-5.4	3.2	3.9	2.0	8.3

GZTD	-0.3	-6.0	5.1	4.2	2.1	8.5
UNB3m	1.2	-6.7	11.2	5.2	2.4	12.2
UNB3	2.6	-6.5	13.4	5.6	2.3	13.7
EGNOS	2.4	-6.6	15.3	5.7	2.4	12.3

As can be seen from Table 3, in terms of the results of accuracy and stability testing for all IGS sites throughout the year, GZTD2 model performs with the best average RMS, and then GZTD model follows. Global correction accuracy of the new model reaches centimeter level: Bias average value is -0.3 cm, average RMS is 3.9 cm. Compared with GZTD model, the range of Bias of GZTD2 model reduce by 2.4 cm and the maximum RMS of GZTD2 model decreases by 0.2 cm, indicating that the new model has a higher stability. Bias and RMS of EGNOS model are very close to those of UNB3 model and both are worse than UNB3m, which is similar to the results of Li et al. (2012). To display the correction effects of different models in a more intuitive way, we computed the distributions of Bias and RMS of all IGS stations. Figure 7 shows the histograms of Bias and RMS for the three models.

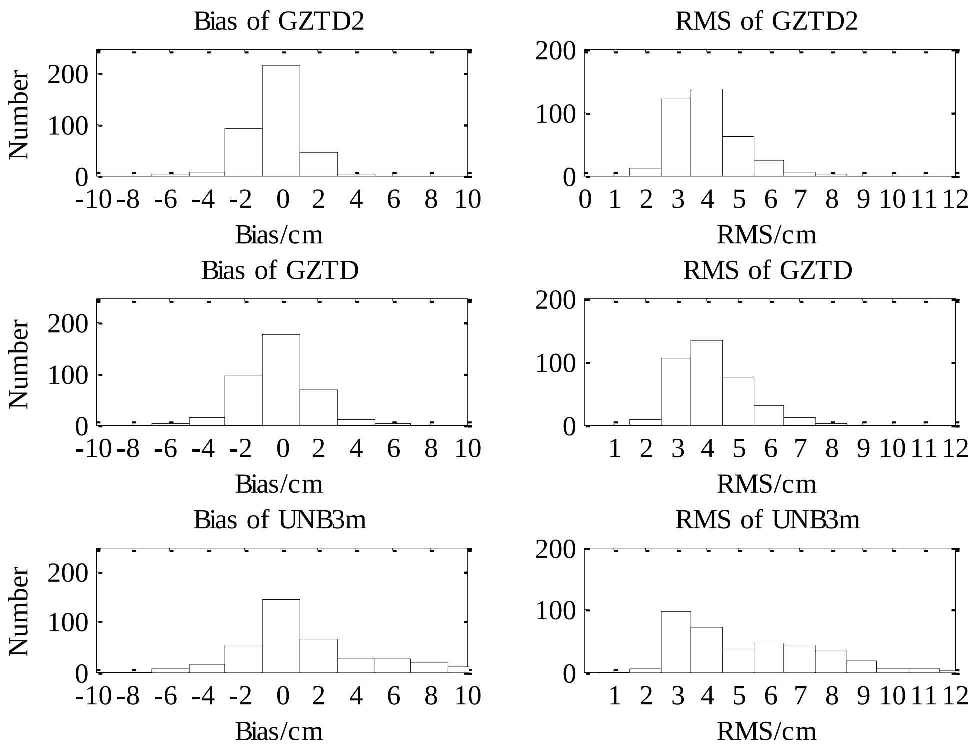

Figure 7. Histograms of Bias and RMS for three models

As can be seen from Figure 7, the Bias of GZTD2 model concentrates in range of [-3cm 3cm], while the main distribution range of the Bias of GZTD model are 1cm larger, and the Bias for UNB3m is distributed with the range more than 8 cm. It indicates that GZTD2 model and GZTD model have small systematic deviations compared with IGS data on a global scale, with the former performing better than the latter, but problematic systematic deviations exist in the UNB3m model within some special areas. Figure 7 also shows that the RMS of GZTD2 model is mostly around 4 cm, whose distribution is more concentrated compared to GZTD model, indicating GZTD2 model has higher stability than GZTD. The RMS of UNB3m model are mainly around 5 cm and exceed 9 cm at many sites, which further suggests the existence of systematic deviations in certain areas in the UNB3m model.

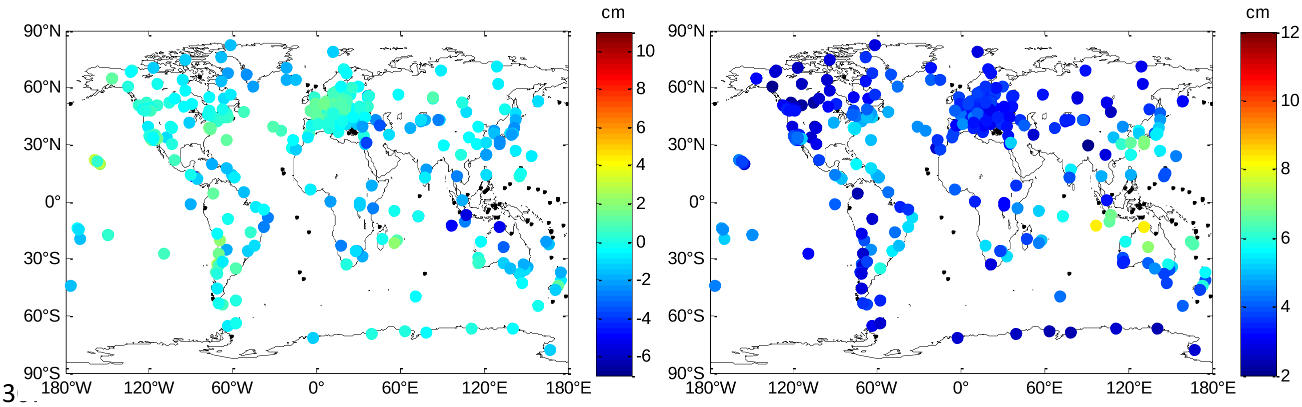

(a) GZTD2 Bias (b) GZTD2 RMS

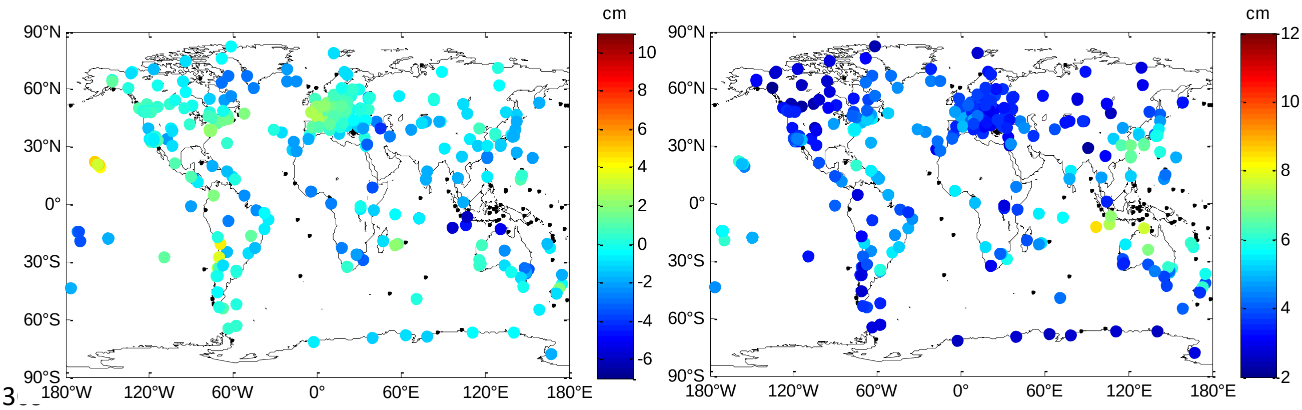

(c) GZTD Bias (d) GZTD RMS

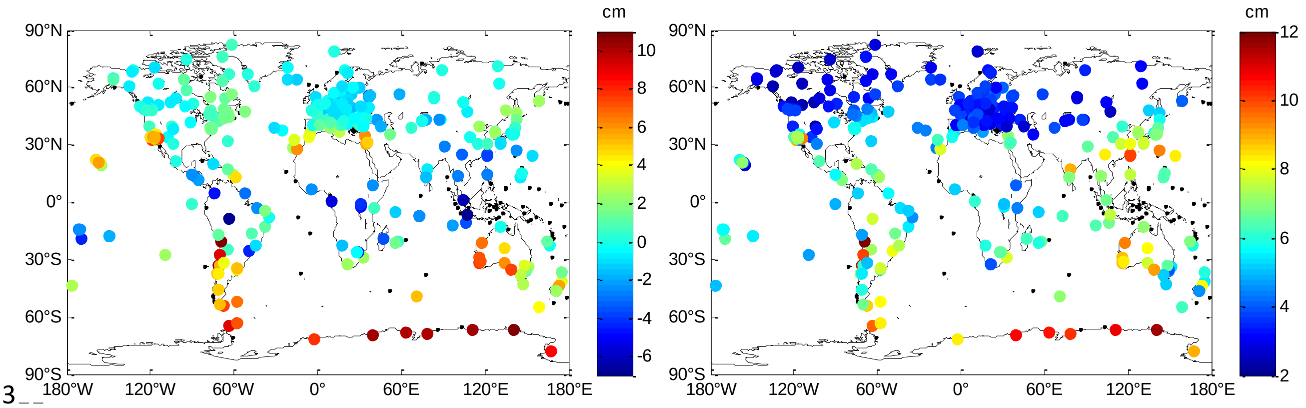

(e) UNB3m Bias (f) UNB3m RMS

Figure 8. Global distributions of Bias and RMS for different models

To further analyze the accuracy of the different models varying with location, Figure 8 shows the global distributions of Bias and RMS calculated from different models for IGS sites. As can be seen from Figure 8, GZTD2 and GZTD model largely eliminate the effects caused by latitude and longitude variations, and the former is more stable than the latter in terms of global distribution of Bias and RMS in spite of a few sites with relative large error, of which most sites are located in the ocean and seacoast areas. A more clear comparison in terms of RMS between GZTD and GZTD2 is shown in Figure 9.The reduction for RMS can be found at most sites (the number is 273) when moving from GZTD to GZTD2, which account for 75.4% of all sites. The significant improvements of RMS are found at the sites in low-latitude areas such as Pacific Ocean, South America coast and West Africa coast where the diurnal variations are notable (see Figure 3d). This result proves the reasonability of adding diurnal variations in GZTD2. For UNB3m model, as it is presented in Figure 8 Biases are negative in most parts of the Northern Hemisphere and positive in most parts of the Southern Hemisphere with significantly larger deviations, and RMS are smaller for areas in the latitudes higher than 30 degrees, again suggesting that the correction effect of UNB3m model is regional.

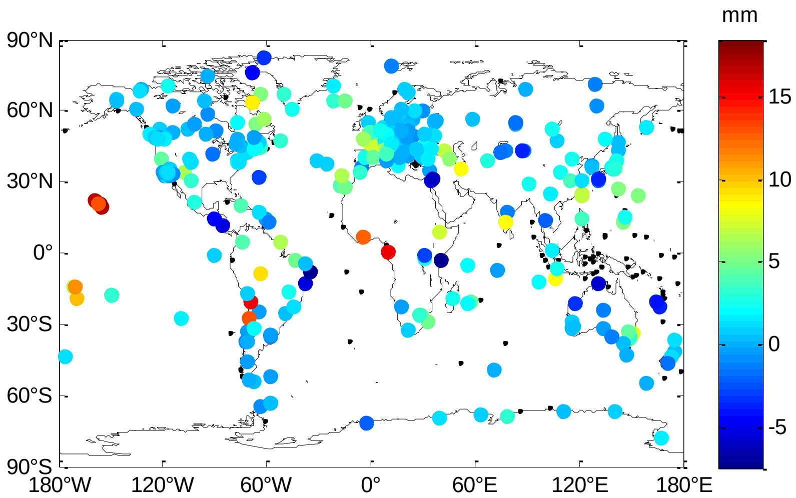

Figure 9. Global distribution of the difference between GZTD's RMS and GZTD2's RMS (GZTD's RMS minus GZTD2's RMS)

Figure 10 shows the global distribution of Bias and RMS with respect to height for GZTD2 model, GZTD model and UNB3m model. As can be seen, the Bias and RMS are larger with height less than 500 m for all three models. Between 500m and 2000m height, the Bias and RMS of GZTD model and GZTD2 model perform better than that of UNB3m model, and the overall correction effects of the GZTD and GZTD2 model are also better than the latter. Due to the same exponential function and reducing constant for height, the distribution patterns of the Bias and RMS of GZTD and GZTD2 model with respect to height are roughly similar, but the latter is obviously superior to the former.

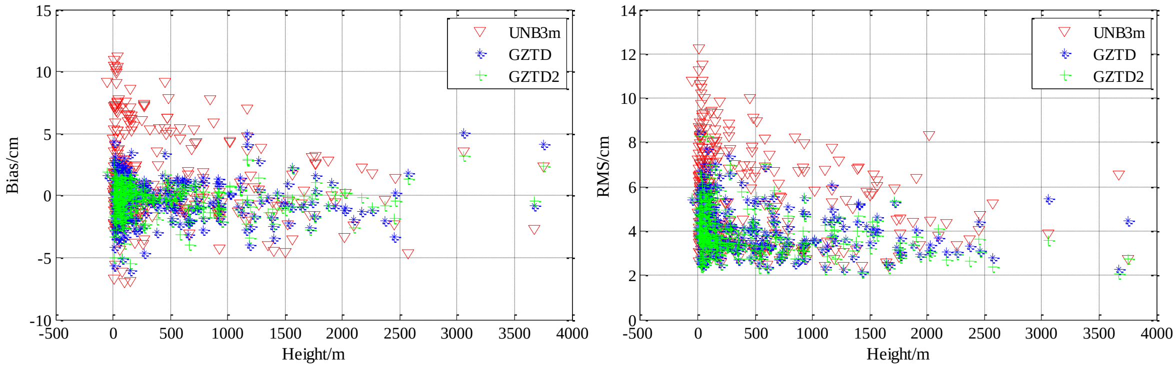

Figure 10. Global distributions of Bias and RMS for different models with respect to height

For a more comprehensive analysis of the relationship between model stability and height, Figure 11 presents the global distribution of relative RMS for three models with respect to height. The relative RMS is the ratio of the RMS to the annual mean ZTD at the site. Basically, a relative accuracy between 1% and 2.5% can usually be stated for the majority of the sites from GZTD2 model, and the relative accuracy is less than 3% for GZTD model, showing that both perform better than UNB3m model.

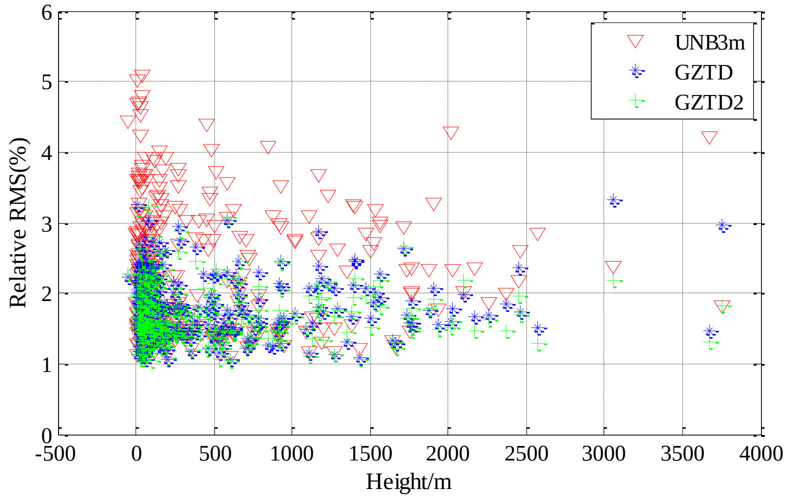

Figure 11. Relative RMS for different models with respect to height

Figure 12 illustrates the comparisons between IGS ZTD data and ZTDs determined by UNB3m, GZTD and GZTD2 models over the year 2010 at site KOUR and TWTF. During the whole year 2010, the ZTD values estimated by GZTD2 model show the best agreement with the IGS data, which are better than that of GZTD model without diurnal terms. The ZTDs determined by UNB3m model vary slightly throughout the year 2010, thus resulting in poor performance. The results in Figure 12 indicates that GZTD2 model has a temporal stability for correction accuracy.

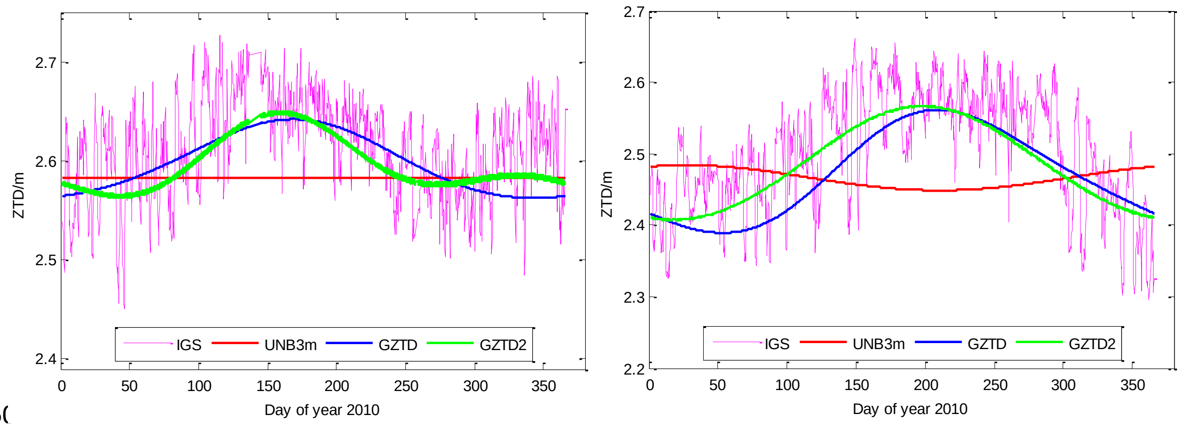

Figure 12. ZTDs at site KOUR (5.3 °N, 52.8 °W, 9.5m; left) and TWTF (24.9 °N, 121.2 °E, 189.9m; right) as provided by IGS and as estimated by different models over year 2010

From the above analysis, we can conclude that the overall accuracy of GZTD2 model is up to centimeter level. GZTD2 model is substantially superior to other commonly used models in terms of Bias and RMS, and the accuracy improves significantly compared with GZTD model, thus performing a higher reliability and stability.

4. Conclusions

In this paper, using the time series data of global tropospheric zenith delays provided by GGOS Atmosphere, we analyzed the diurnal variation in the ZTD which is neglected in the previous GZTD model, then we modified the model function to develop an improved model named GZTD2. We conducted external validation testing with GGOS ZTD grid data which was not involved in modeling, and IGS tropospheric product. The testing results of GGOS ZTD grid data show that the global average Bias and RMS for GZTD2 model are 0.2 cm and 3.8 cm respectively. The global average Bias is comparable to that of GZTD model, but the global average RMS has been reduced by 0.3 cm. Both the Bias and RMS are far better than EGNOS model and the UNB series models. The testing results of global IGS tropospheric product show that the Bias and RMS for GZTD2 model are -0.3 cm and 3.9 cm, superior to those of GZTD (-0.3 cm and 4.2 cm), indicating higher accuracy and reliability compared to the EGNOS model and the UNB series models.

Overall, compared to GZTD model, GZTD2 model improves the temporal resolution and spatial resolution by considering diurnal periodic variations and modifying the expansion function, further completing and optimizing the theory of model establishment. The reliability and stability for GZTD2 model are much better than other commonly used models. However, like other empirical models such as UNB3m, GZTD2 model would be inaccurate in extreme weather events. Saastamoinen model is recommended if the real-time meteorological observations are available under extreme weather events. Moreover, GZTD2 model doesn't consider the semidiurnal variations due to the temporal resolution of GGOS data. In order to build a global tropospheric model with high accuracy, ZTD data with high quality and resolution are required, and the diurnal and semidiurnal variations as well as the subtle secular variation trend of ZTD need more detailed and further study.

Acknowledgements *The authors would like to express gratitude toward GGOS Atmosphere for providing related data. Great appreciation also goes to IGS for their data supporting of reference tropospheric product. This research was supported by the National Natural Science Foundation of China (41174012; 41274022) and The National High Technology Research and Development Program of China (2013AA122502) and the Fundamental Research Funds for the Central Universities (2014214020202) and the Surveying and Mapping Basic Research Program of National Administration of Surveying, Mapping and Geoinformation (13-02-09).*

References

Black H D (1978). An easily implemented algorithm for the tropospheric range correction. *Journal of Geophysical Research: Solid Earth (1978–2012)*, **83**(B4), 1825-1828.

Böhm, J., Heinkelmann, R., & Schuh, H. (2007). Short note: a global model of pressure and temperature for geodetic applications. *Journal of Geodesy*, **81**(10), 679-683.

Böhm, J., & Schuh, H. (eds.) (2013). *Atmospheric Effects in Space Geodesy*, Springer Verlag, ISBN 978-3-642-36931-5.

Böhm, J., Möller, G., Schindelegger, M., Pain, G., & Weber, R. (2015). Development of an improved empirical model for slant delays in the troposphere (GPT2w). *GPS Solutions, 19*(3), 433-441.

Byun, S. H., & Bar-Sever, Y. E. (2009). A new type of troposphere zenith path delay product of the international GNSS service. *Journal of Geodesy*, **83**(3-4), 1-7.

Collins J P, Langley R B(1997). *A tropospheric delay model for the user of the wide area augmentation system. Department of Geodesy and Geomatics Engineering*, University of New Brunswick.

Collins, J. P., & Langley, R. (1998, September). The residual tropospheric propagation delay: How bad can it get? In *PROCEEDINGS OF ION GPS* (Vol. 11, pp. 729-738). INSTITUTE OF NAVIGATION.

Dodson A H, Chen W, Baker H C, Penna N T, Roberts G W, Jeans R J, Westbrook J(1999). Assessment of EGNOS tropospheric correction model. In *Proceedings of the 12th International Technical Meeting of the Satellite Division of The Institute of Navigation (ION GPS 1999)* (pp. 1401-1408).

Hopfield H S (1969). Two‐quartic tropospheric refractivity profile for correcting satellite data. *Journal of Geophysical research*, **74**(18), 4487-4499.

Jin, S., Park, J. U., Cho, J. H., & Park, P. H. (2007). Seasonal variability of GPS‐derived zenith tropospheric delay (1994–2006) and climate implications. *Journal of Geophysical Research: Atmospheres (1984–2012)*, 112(D9).

Jin, S., Luo, O. F., & Gleason, S. (2009). Characterization of diurnal cycles in ZTD from a decade of global GPS observations. *Journal of Geodesy*, **83**(6), 537-545.

Krueger E, Schueler T, Hein G W, Martellucci A, Blarzino G(2004, May). Galileo tropospheric correction approaches developed within GSTB-V1. In *Proc. ENC-GNSS*.

Krueger E, Schueler T, Arbesser-Rastburg B(2005). The standard tropospheric correction model for the European satellite navigation system Galileo. *Proc. General Assembly URSI*.

Lagler, K., Schindelegger, M., Böhm, J., Krásná, H., & Nilsson, T. (2013). GPT2: Empirical slant delay model for radio space geodetic techniques.*Geophysical research letters*, *40*(6), 1069-1073.

Leandro R, Santos M C, Langley R B(2006, January). UNB neutral atmosphere models: development and performance. In *ION NTM* (pp. 18-20).

Leandro R F, Langley R B, Santos M C(2008). UNB3m_pack: a neutral atmosphere delay package for radiometric space techniques. *GPS Solutions*, **12**(1), 65-70.

Li Wei, Yuan Y B, Ou J K, Li H, Li Z S(2012). A new global zenith tropospheric delay model IGGtrop for GNSS applications. *Chinese Science Bulletin*, **57**(17), 2132-2139.

Li, Wei, Yuan, Y., Ou, J., Chai, Y., Li, Z., Liou, Y. A., & Wang, N. (2015). New versions of the BDS/GNSS zenith tropospheric delay model IGGtrop.*Journal of Geodesy*, *89*(1), 73-80.

Möller, G., Weber, R., & Böhm, J. (2014). Improved troposphere blind models based on numerical weather data. *Navigation*, *61*(3), 203-211.

Penna N, Dodson A, Chen W(2001). Assessment of EGNOS tropospheric correction model. *The*

Journal of Navigation, **54**(01), 37-55.
Pramualsakdikul, S., Haas, R., Elgered, G., & Scherneck, H. G. (2007). Sensing of diurnal and semi‐diurnal variability in the water vapour content in the tropics using GPS measurements. Meteorological Applications, 14(4), 403-412.
Saastamoinen J (1973). Contributions to the theory of atmospheric refraction. *Bulletin Géodésique (1946-1975)*, **107**(1), 13-34.
Schüler T (2014). The TropGrid2 standard tropospheric correction model. *GPS solutions*, **18**(1), 123-131.
Spilker, J. J. (1980). GPS signal structure and performance characteristics.*Global positioning system*, *1*, 29-54.
Trenberth, K. E., Fasullo, J., & Smith, L. (2005). Trends and variability in column-integrated atmospheric water vapor. Climate Dynamics, 24(7-8), 741-758.
Ueno M, Hoshinoo K, Matsunaga K, Kawai M, Nakao H, Langley R B, Bisnath S B (2001, January). Assessment of atmospheric delay correction models for the Japanese MSAS. In *Proceedings of the 14th International Technical Meeting of the Satellite Division of The Institute of Navigation (ION GPS 2001)* (pp. 2341-2350).
Uppala S M, Kållberg P W, Simmons A J, Andrae U, Bechtold V, Fiorino M, ... ,Woollen J (2005). The ERA‐40 re‐analysis. *Quarterly Journal of the Royal Meteorological Society*, **131**(612), 2961-3012.
Yao Y B, He C Y, Zhang B, Xu C Q(2013). A new global zenith tropospheric delay model GZTD. *Chinese Journal of Geophysics-Chinese Edition*, **56**(7), 2218-2227,doi:10.6038/cjg20130709